catalysts

Article

Synergistic Effect of Photocatalytic Degradation of Hexabromocyclododecane in Water by UV/TiO_2/persulfate

Qiang Li [1,2], Lifang Wang [1], Xuhui Fang [3], Li Zhang [2,*], Jingjiu Li [2] and Hongyong Xie [2,*]

[1] School of Management, Northwestern Polytechnical University, 127 West Youxi Road, Xian 710072, China; failureend@163.com (Q.L.); lifang@nwpu.edu.cn (L.W.)
[2] Research Center of Resource Recycling Science and Engineering, School of Environmental and Materials Engineering, Shanghai Polytechnic University, Shanghai 201209, China; lijingjiu123@163.com
[3] Centre Testing International Pinbiao (Shanghai) Co., Ltd., 1996 New Jinqiao Road, Shanghai 201206, China; fangxuwh@126.com
* Correspondence: zhangli@sspu.edu.cn (L.Z.); hyxie@sspu.edu.cn (H.X.); Tel.: +86-021-5021-1210 (L.Z.); +86-021-5021-1231 (H.X.)

Received: 4 January 2019; Accepted: 31 January 2019; Published: 18 February 2019

Abstract: In this work, the elimination of hexabromocyclododecane (HBCD) is explored by using photodegradation of the UV/TiO_2 system, the UV/potassium persulfate (KPS) system, and the homo/heterogeneous UV/TiO_2/KPS system. The experimental results show that the dosages of TiO_2 and potassium persulfate have optimum values to increase the degradation degree. HBCD can be almost completely degraded and 74.3% of the total bromine content is achieved in the UV/TiO_2/KPS homo/heterogeneous photocatalysis, much more than in the UV/persulfate system and the UV/TiO_2 system. Roles of radicals $SO_4^{\bullet-}$ and $OH^{\bullet}$ in the photocatalysis systems are discussed based on experimental measurements. The high yield of the concentration of bromide ions and decreased pH value indicates that synergistic effects exist in the UV/TiO_2/KPS homo/heterogeneous photocatalysis, which can mineralize HBCD into inorganic small molecules like carboxylic acids, CO_2 and H_2O, thus much less intermediates are formed. The possible pathways of degradation of HBCD in the UV/TiO_2/KPS system were also analyzed by GC/MS. This work will have practical application potential in the fields of pollution control and environmental management.

Keywords: hexabromocyclododecane; environmental management; photocatalysis; advanced oxidation processes

1. Introduction

Hexabromocyclododecane (HBCD) is a high bromine content additive flame retardant that is mainly used in polystyrene electrical equipment, insulation boards, resin, polyester fabric, synthetic rubber coating, and so on [1]. Studies have shown that HBCD is a potential endocrine disruptor, and it has immunotoxicity, neurotoxicity, and cytotoxicity [2]. The presence of HBCD was detected in environmental samples such as water, atmosphere, sediment, soil, food, and even in the human body in breast milk and plasma, as it can be enriched through the food chain, causing persistent pollution [3]. The hazard of HBCD and its pollution in the environment have caused widespread concern, and it is of great significance to develop a strategy for the elimination of HBCD pollution [4]. However, the molecular structure of HBCD with a ring structure is relatively stable, making it heat-resistant, UV-resistant, and difficult to be decomposed in the natural environment [5]. Methods for eliminating HBCD in the environment include microbial degradation, ultrasonic degradation, chemical reduction, phytoremediation, and mechanical ball milling [6–8]. However, these methods have not been practically used because of the harsh reaction conditions, high energy consumption, low efficiency, and secondary pollution [9,10]. Nowadays, advanced oxidation processes (AOPs) have been widely used for the elimination of organic pollutants of water or gas, using the highly reactive chemical species like hydroxyl radicals ($OH^\bullet$) to oxidize most of pollutants into small molecular substances that are harmless to the environment, such as CO_2, H_2O and so on [11]. Increasing the number of hydroxyl radicals could increase the efficiency of the AOPs reactions. Some types of AOPs based on UV, H_2O_2/UV, O_3/UV and H_2O_2/O_3/UV combinations use photolysis of H_2O_2 and ozone to produce $OH^\bullet$, while the heterogeneous UV/TiO_2 photocatalysis and homogeneous photo-Fenton are based on the use of a wide-band gap semiconductor and addition of H_2O_2 to dissolved iron salts that produce $OH^\bullet$ under UV irradiation, respectively [12]. Among AOPs, the UV/TiO_2 heterogeneous photocatalysis has gradually attracted the interest of scientists in elimination of toxic pollutions due to its efficiency, low-cost and broad applicability [13]. The photocatalytic technology can be briefly described as follows: under UV irradiation, the electron in TiO_2 was excited and transferred from the valence band (VB) to the conduction band (CB), resulting in the formation of high energy electron-hole pairs; the electrons may also react with O_2 and generate a superoxide ion ($O_2^{\bullet -}$), while holes were captured by surface hydroxyl groups (OH^-) on the photocatalyst surface to yield $OH^\bullet$ [14,15]. However, the photogenerated electron-hole pairs are easy to combine within a very short time of 10^{-9}~10^{-12} s, which results in a lower photocatalytic degradation efficiency [16]. In order to solve this problem, scientists have conducted lots of meaningful and in-depth research. For instance, Aronne et al. found that high Ti^{3+} self-doping TiO_{2-x} not only has a wide range of visible light responses, but also has a low recombination rate of electron–hole pairs [17]; Sannino et al. fabricated hybrid TiO_2–acetylacetonate amorphous gel-derived material with stably adsorbed superoxide radical ($O_2^{\bullet -}$) active in oxidative degradation of organic pollutants in the absence of any light irradiation [18,19].

It has been reported that using the strong oxidant of persulfate ion ($S_2O_8^{2-}$) (with redox potential of 2.05 V) is effective for degrading organic pollutions in water solution through direct chemical oxidation [20]. The $S_2O8_2^-$ can be activated via thermal, UV light, or redox decomposition to generate the stronger oxidant of sulfate radicals (E_0 = (2.5–3.1) V vs. NHE) [21–23]. It's worthwhile to note that both the persulfate ion and sulfate radicals ($SO_4^{\bullet -}$) can be dissolved in water, so the free radicals and contaminants in water can be contracted at the molecular level, leading to a higher reaction rate. For instance, Li et al. have found that addition of persulphate to UV/TiO_2 could improve the photocatalytic degradation of tetrabromobisphenol A and other pollutants [24–26]. Therefore, it is necessary to combine persulfate and UV/TiO_2 photocatalytic techniques to increase the mineralization of HBCD.

In this work, degradation of HBCD under UV/TiO_2, UV/potassium persulfate (KPS), and UV/TiO_2/KPS systems were investigated. Effects of TiO_2 and KPS dosage have been examined on degradation degree of HBCD. The photodegradation efficiency and the yield of bromide ion were tested to evaluate the mineralization of HBCD. The intermediates were analyzed by GC/MS to study the degradation mechanism. Based on experimental measurements, roles of radicals $SO_4^{\bullet -}$ and $OH^\bullet$ in the photocatalysis systems were also discussed.

2. Results and Discussions

2.1. Determination of TiO_2 Dosages

The amount of catalysts added in the solution needs to be matched to the number of contaminants in the photocatalytic process, so the dosing weight range of the catalyst were determined. Figure 1 shows the effects of different TiO_2 dosages on the photodegradation rate of HBCD. Under the condition of no addition of TiO_2, the degradation rate was only 21.5% at 180 min. Having increased the catalyst dosage of TiO_2 to 100 mg/L, the photocatalytic efficiency also increased to 82.93%. Further increasing the dosage of TiO_2 more than 100 mg/L, the photocatalytic efficiency decreased. The dosage of the addition increased the suspended particles in the solution, and greatly reduced the utilization of light, resulting in the partial catalyst not being fully activated during the photocatalysis, so the photocatalytic efficiency decreased [24,27]. In addition, the HBCD adsorbed on the catalysts in dark is less than 10%, so the free radical ($OH^{\bullet}$) reaction dominates the rate of degradation reaction in the UV/TiO_2 system.

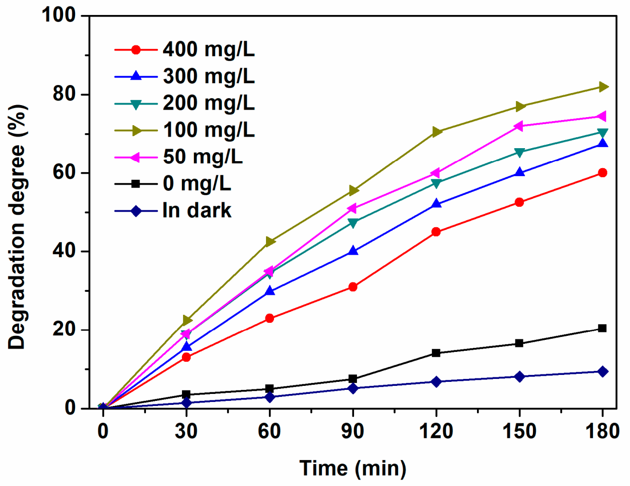

Figure 1. Effects of different TiO_2 dosages on the photodegradation rate of HBCD (the initial concentration of HBCD is 25 mg/L, and KPS dosage is 0 mg/L).

2.2. Effect of KPS Dosage

Figure 2 shows the effect of different $K_2S_2O_8$ dosages on the photodegradation rate of HBCD. The addition of $K_2S_2O_8$ can effectively improve the degradation efficiency of HBCD, but its degradation efficiency increases first and then decreases with further increasing $K_2S_2O_8$ concentration, and the highest degradation efficiency occurs at 4 mM. When the $K_2S_2O_8$ dosage was more than 4 mM, the degradation efficiency of HBCD decreased with the increase of persulfate dosage. When the $K_2S_2O_8$ concentrations in the solution are between 0 and 4 mM, the main reactions in the UV/TiO_2/KPS system are as follows [28]:

$$S_2O_8{}^{2-} + UV \rightarrow 2SO_4{}^{\bullet -} \tag{1}$$

$$TiO_2 + UV \rightarrow e^-_{CB} + h^+_{VB} \tag{2}$$

$$S_2O_8{}^{2-} + e^-_{CB} \rightarrow 2SO_4{}^{\bullet -} \tag{3}$$

$$H_2O + h^+_{VB} \rightarrow OH^{\bullet} + H^+ \tag{4}$$

The advanced oxidation process relies on the amount of free radicals and is reflected in the degradation rate of the contaminants. The strong oxidizing agents of sulfate radicals ($SO_4{}^{\bullet -}$) and hydroxyl radicals ($OH^{\bullet}$) generated by the above reactions increase with increasing KPS concentration in the solution. But increasing the KPS dosage further to 8 mM will lead to a surplus of reactants ($S_2O_8{}^{2-}$), which may deplete lots of $OH^{\bullet}$ and $SO_4{}^{\bullet -}$, and lead to the decrease of the degradation degree by the following two reactions [29]:

$$S_2O_8{}^{2-} + OH^{\bullet} \rightarrow S_2O_8{}^{\bullet -} + OH^- \tag{5}$$

$$S_2O_8{}^{2-} + SO_4{}^{\bullet -} \rightarrow SO_4{}^{2-} + S_2O_8{}^{\bullet -} \tag{6}$$

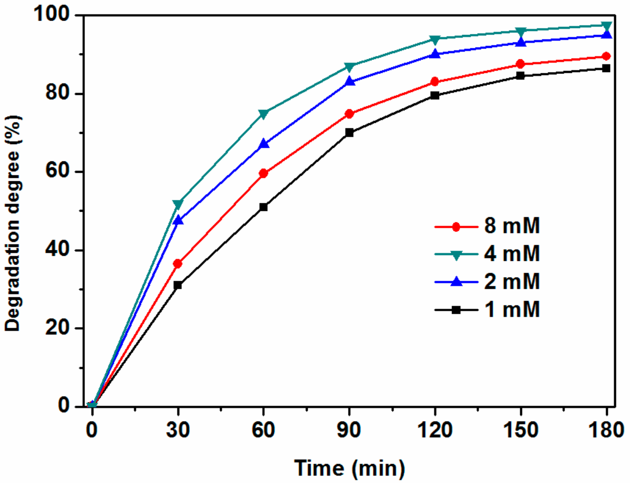

Figure 2. Effects of different KPS dosages on the photodegradation rate of HBCD (the initial concentration of HBCD is 25 mg/L, and TiO_2 dosage is 100 mg/L).

2.3. Kinetic Analysis of Different Reaction Systems

Figure 3 shows the degradation effect of HBCD in the three systems of "UV/TiO_2 (TiO_2: 100 mg/L)", "UV/$K_2S_2O_8$ (KPS: 4 mM)", and "TiO_2 (TiO_2: 100 mg/L) + $K_2S_2O_8$ (KPS: 4 mM)", respectively. The initial HBCD concentration and light source in the three systems were all the same (25 mg/L, 100 W mercury lamp). The degradation degree of HBCD over time in 180 min is shown in Figure 3a. The degradation degree for the UV/TiO_2/KPS photocatalytic system was 87.6% at 90 min, but the degradation rates for the UV/TiO_2 photocatalytic system and UV/KPS system were only 56.8% and 52.5% at the same time. The above experimental results show that the degradation effect of UV/TiO_2/KPS photocatalytic system on HBCD is far superior to that of the UV/TiO_2 system and the UV/KPS system.

The kinetic model was used to study the degradation dynamic behavior of the three different systems [30], $-\ln(C_0/C) = kt$, where k is the reaction apparent rate constant and t is the light irradiation time. Figure 3b shows the effect of different systems on the kinetics of HBCD under irradiation for 180 min. The three reaction systems are all fit to pseudo-first-order kinetics, and the k values for the UV/KPS system, the UV/TiO_2 system, and the UV/TiO_2/KPS system are 0.0065, 0.0080, and 0.0174 min^{-1}, respectively (Figure 3b). Obviously, the k value of the UV/TiO_2/KPS system is far higher than those of the UV/KPS system and the UV/TiO_2 system, indicating that the degradation efficiency of the UV/TiO_2/KPS photocatalytic system is much higher than that of the UV/KPS photocatalytic system and the UV/TiO_2 photocatalytic system. The photocatalytic process of the UV/TiO_2 system contains an adsorption and free radical ($O_2^{\bullet-}$, $OH^{\bullet}$, etc.) reaction [21]. The HBCD adsorbed on the catalysts in dark is less than 10%, so the free radical reaction dominates the rate of degradation reaction in the UV/TiO_2 system. The UV/KPS system also relies on sulfate radicals ($SO_4^{\bullet-}$, $S_2O_8^{\bullet-}$, etc.) excited by UV light to degrade pollutants [22,24]. In the UV/TiO_2/KPS system, more free radicals were present and the free radical reaction is more complicated. $S_2O_8^{2-}$ can be excited by photogenerated electrons on the surface of the catalyst to generate sulfate radicals ($SO_4^{\bullet-}$), while $SO_4^{\bullet-}$ can react with OH^- to produce $OH^{\bullet}$ [21–24]. In the three systems, the degradation rates are all determined by the reactions between free radicals and contaminant molecules, while the intensity of the UV light (100 W) and the initial concentration (25.00 mg/L) of the contaminants in the three systems are all the same, so all reaction systems could be in line with pseudo-first-order kinetics. Figure S1 (Supporting Information) shows the degradation of HBCD over the UV/TiO_2/KPS system with three time cycling uses. The TiO_2 photocatalysts could be easily recovered by sedimentation and reused, which would greatly promote their industrial application in eliminating organic pollutants from wastewater.

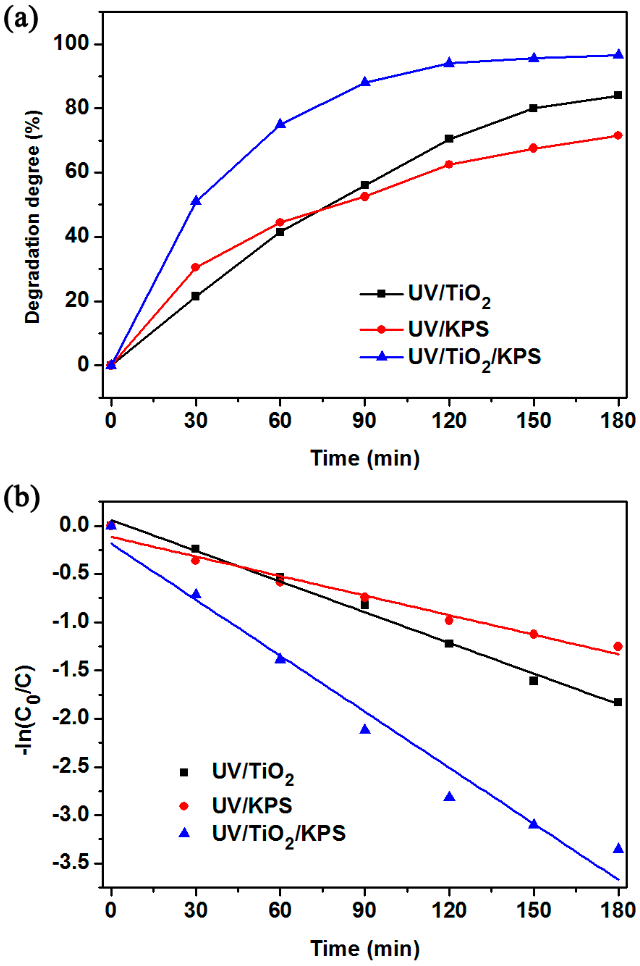

Figure 3. The degradation degree (**a**) and kinetic linear simulation curves of the removal of HBCD (**b**) in UV/TiO_2, UV/KPS, and UV/TiO_2/KPS systems. (The initial concentration of HBCD is 25.0 mg/L, KPS dosage is 4 mg/L, and TiO_2 dosage is 100 mg/L).

2.4. The Mineralization Degree of HBCD

Measuring the concentration of bromide ion is a practical strategy to evaluate the amount of intermediates and the mineralization degree of HBCD [24]. Figure 4 shows the change of bromide ion concentration during the degradation of HBCD in the UV/TiO_2/KPS system. The initial HBCD concentration, TiO_2 dosage, and $K_2S_2O_8$ dosage were 25.0 mg/L, 100 mg/L, and 4 mM, respectively.

As can be seen from Figure 4, with the prolongation of degradation time, the concentration of bromide ion in the solution increased continuously. When the reaction was carried out for 3.0 h, the concentration of bromide ions in the solution was 13.8 mg/L, which accounted for 74.3% of the total bromine content of HBCD in the solution. It can be seen that the yield of bromine ion by UV/TiO_2/KPS system is much better than that of UV/TiO_2 system (12.3 mg/L) and UV/KPS system (11.9 mg/L). The significantly increased bromide ion concentration yield indicates that there exist synergistic effects in the UV/TiO_2/KPS photocatalysis as described in the previous Formulas (1)–(4), which can mineralize HBCD into inorganic small molecules relatively thorough, thus much fewer intermediates are formed in UV/TiO_2/KPS homo/heterogeneous photocatalysis.

Figure 5 shows the change of pH in solution over time during HBCD degradation. It can be seen that the pH value of the solution gradually decreases from 6.53 to 3.72 with the increasing of the degradation time within 180 min. It may be due to the partial consumption of OH^- in the solution, since OH^- can easily react with $SO_4^{\bullet-}$ to produce $OH^\bullet$. The CO_2 gas generated during the mineralization of HBCD subsequently dissolved in the water, which also lead to a decrease in pH.

At the same time, there are some small molecules of carboxylic acids generated in the degradation of HBCD, which also cause the decrease in pH. As mentioned above, the degradation rate of HBCD reached 96.5% when the reaction proceeded to 180 min. It is indicated that the intermediate in the solution is rapidly decomposed into small molecular of carboxylic acids, and further mineralized to CO_2 and H_2O, so that the pH of the solution continued to decrease as the reaction time prolonged. The increasing concentration of bromide ions in the solution and the decreasing pH value indicate that HBCD is highly mineralized in UV/TiO_2/KPS homo/heterogeneous photocatalysis.

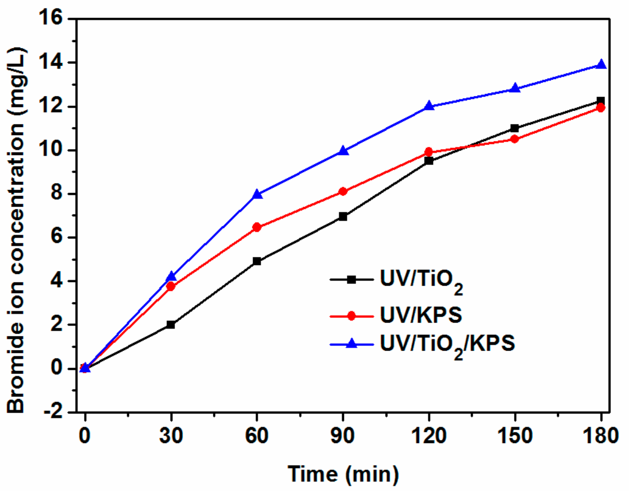

Figure 4. The change of bromide ion in water samples from different time points (the initial concentration of HBCD is 25.0 mg/L, KPS dosage is 4 mg/L, and TiO_2 dosage is 100 mg/L).

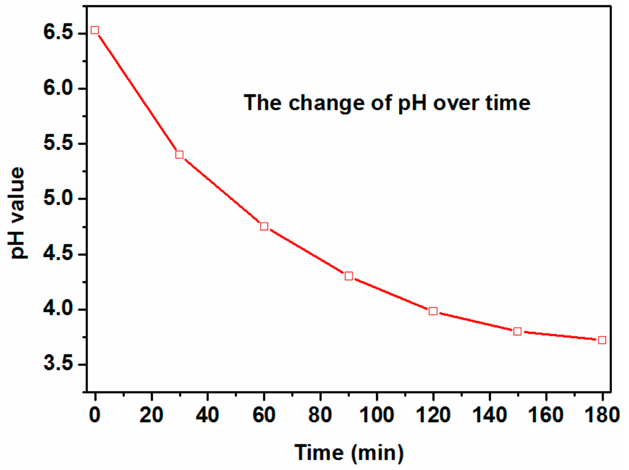

Figure 5. The change of pH over time (the initial concentration of HBCD is 25.0 mg/L, KPS dosage is 4 mg/L, and TiO_2 dosage is 100 mg/L).

2.5. The Mechanism of Photodegradation of HBCD

Figure 6 shows the mass spectrum of the intermediates obtained by GC-MS analysis. The solution was sampled during the degradation of HBCD in the UV/TiO_2/KPS system at 90 min, with the reaction conditions the same as mentioned above. The mass spectrum of degradation products were tetrabromocyclododecene (A), dibromocyclododecadiene (B), 1,5,9-Cyclododecatriene (C), 1,2-Epoxy-5,9-cyclododecadiene (D), dibromo-epoxy-cyclododecene (E), 4,5-dibromooctanedioic acid (F), and succinic acid (G), respectively [31–33].

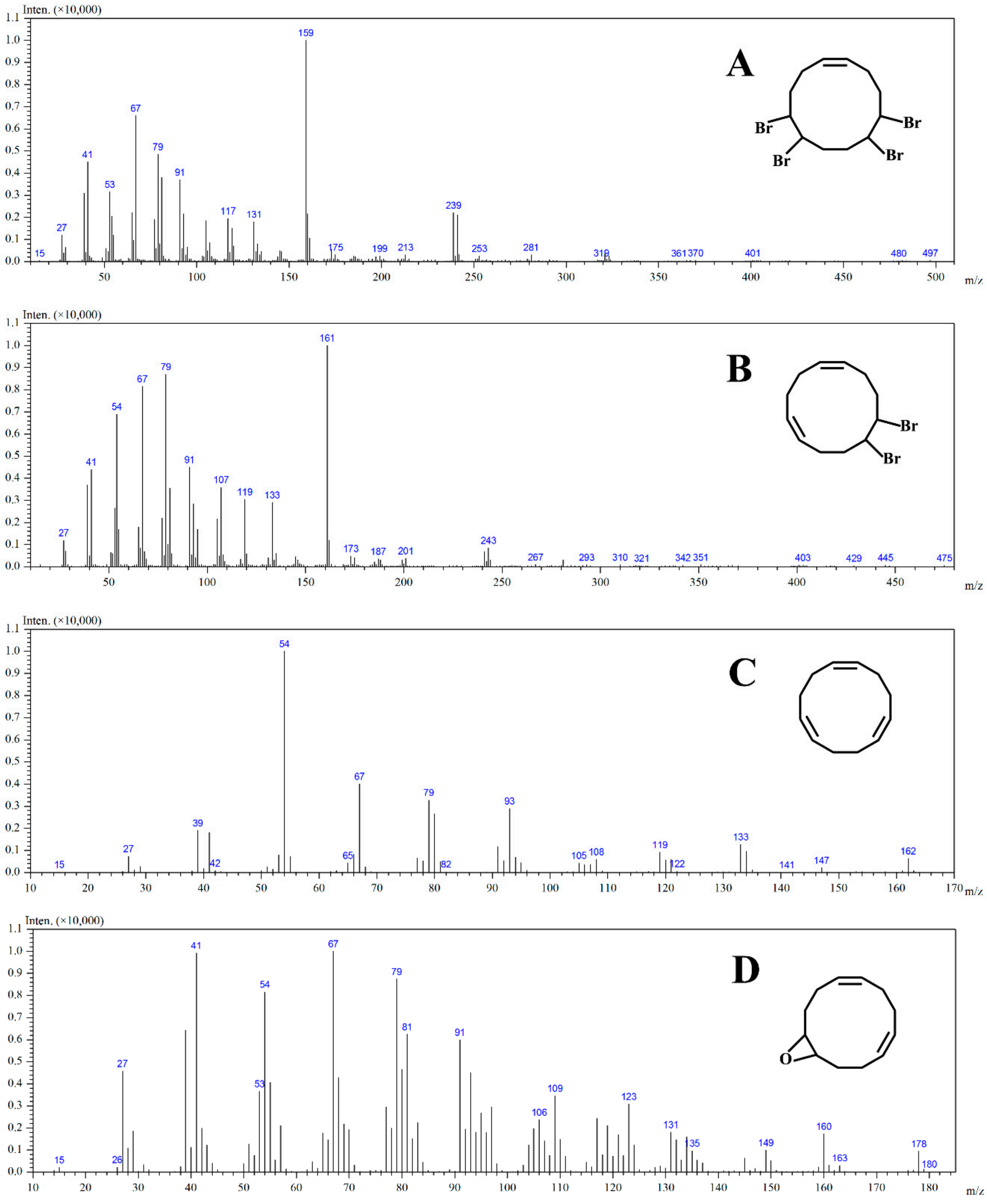

Figure 6. *Cont.*

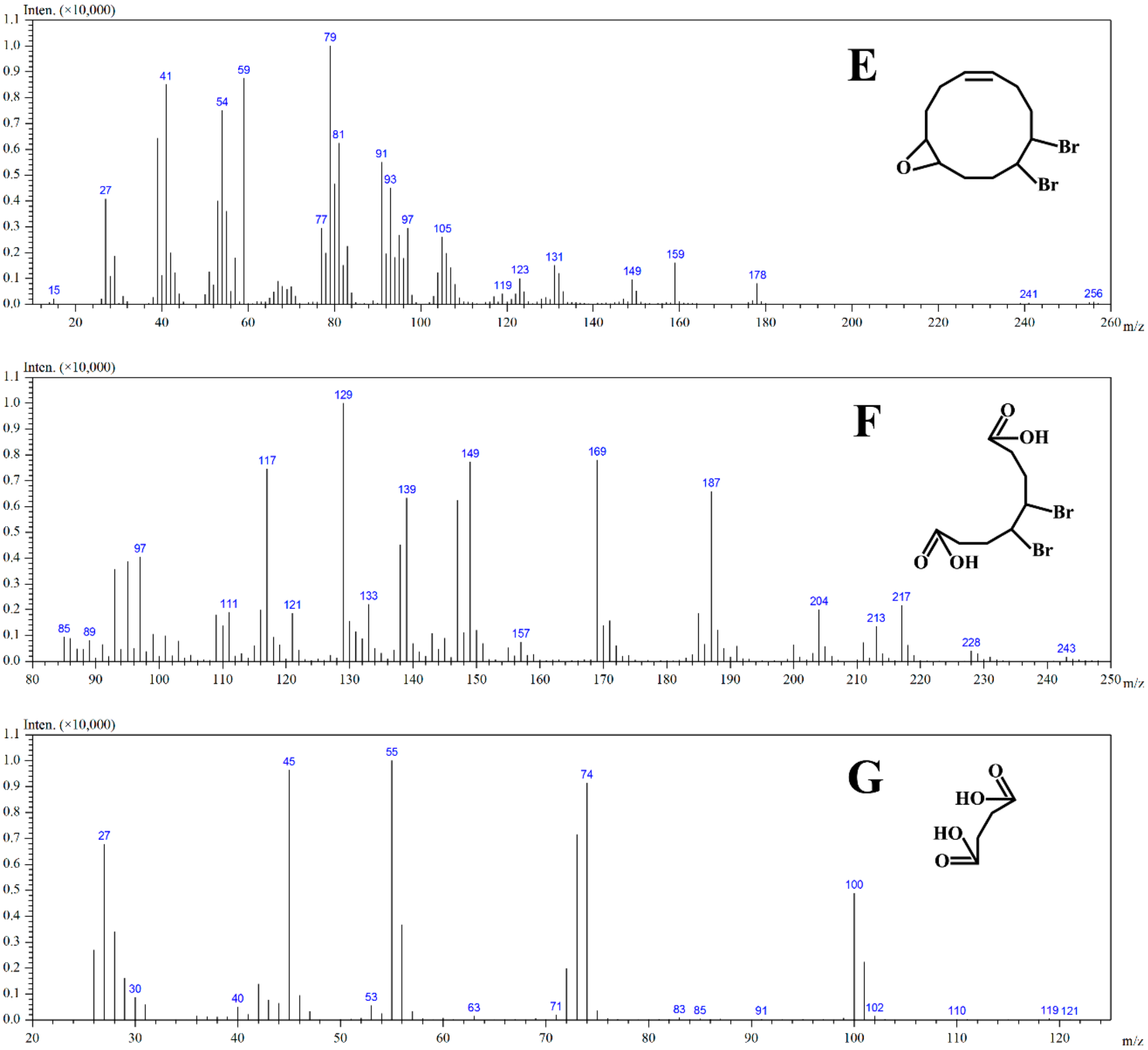

Figure 6. The mass spectrum of the intermediates in the UV/TiO_2/KPS system at 90 min ((**A**) Tetrabromocyclododecene; (**B**) Dibromocyclododecadiene; (**C**) 1,5,9-Cyclododecatriene; (**D**) 1,2-Epoxy-5,9-cyclododecadiene; (**E**) Dibromo-epoxy-cyclododecene; (**F**) 4,5-dibromooctanedioic acid; (**G**) succinic acid).

By analyzing the degradation products of GC/MS, the possible degradation pathway of HBCD in UV/TiO_2/KPS system is determined, as shown in Figure 7. Under the action of active free radicals, two adjacent C–Br bonds in the molecular structure of HBCD undergo cleavage and debromination to form carbon-carbon double bonds, thus the compounds A, B, and C were obtained successively [34]. Compound C can be directly oxidized to D or oxidized to G by double bond cleavage. In addition, the compound B can also be oxidized to form the compound E, or oxidized to F and G by double bond cleavage [35]. The compound F can also be further debrominated and oxidized to form G. Succinic acid (G) is a small molecule, and it can be easily degraded by free radicals (like $SO_4^{\bullet -}$ and $OH^{\bullet}$) into carboxylic acids, CO_2, and H_2O in the following time. The adsorption of intermediate species on the surface of TiO_2 may cover the active sites, which may result in a decrease in catalytic efficiency. But in this work, the initial concentration of HBCD is very low (25 mg/L), and under the irradiation of UV irradiation, the surface of the titanium dioxide is hydrophilic, so the organic intermediates are more easily dispersed into the water-methanol mixed solution under strong stirring.

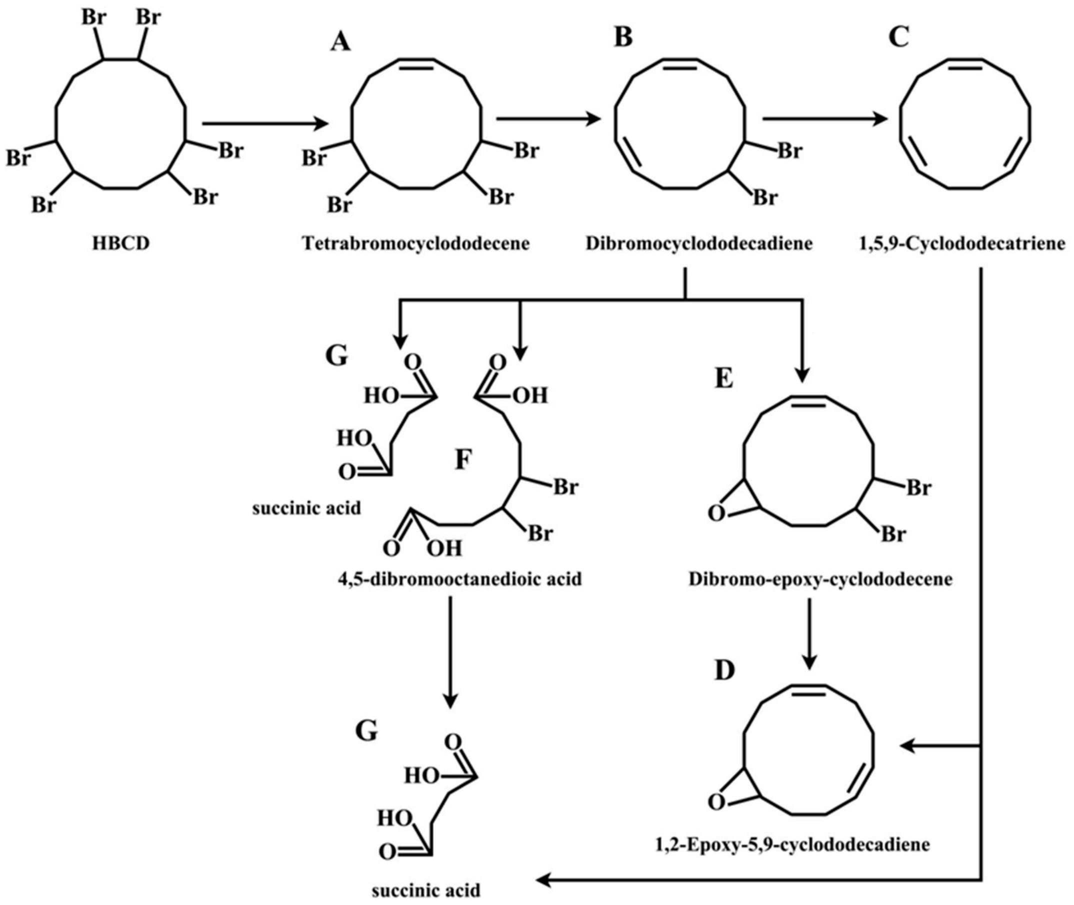

Figure 7. Possible pathways of degradation of HBCD in UV/TiO_2/KPS systems.

3. Materials and Methods

3.1. Reagents

Ethanol (HPLC grade) and acetonitrile (HPLC grade) were supplied by LABSCIENCE (Reno, NV, USA) and TEDIA (Nashville, TN, USA), respectively. HBCD (99.0%), sodium carbonate (99.8%), sodium bicarbonate (99.5%), sodium nitrite (99.0%), potassium persulfate (KPS, 99%), dichloromethane (HPLC grade), anhydrous sodium sulfate (99.0%) and methanol (HPLC grade) were supplied by Sinopharm Chemical Reagent Co., Ltd (Shanghai, China). All reagents were used as received without further purification. TiO_2 nanoparticles were laboratory-made, as described in the previous literature [26].

The preparation of HBCD stock solution was as follows: accurately weigh 0.05 g of HBCD powder into 100 mL volumetric flasks, and add chromatographically pure methanol to the 100 mL mark. After dissolving, the HBCD stock solution with the concentrations of 500.00 mg/L was obtained, and then it was stored in a refrigerator at 4 °C for later use. The HBCD stock solution was diluted by ultrapure water to different concentrations for drawing the peak area-concentration standard curve, and it also be used as pollutants in the photodegradation experiments.

3.2. Photodegradation of HBCD

The photoreactor was supplied by Xujiang Electromechanical Plant (XPA-7, Nanjing, China). For determination of TiO_2 dosages, a 50 mL HBCD water-methanol mixture solution with the concentration of 25.00 mg/L was added into a quartz tube, and then TiO_2 powder with different dosages (0~400 mg/L) were also added into the tube. For determination of the effect of KPS dosage, a 50 mL HBCD water-methanol mixture solution with the concentration of 25.00 mg/L was added into a quartz tube, and then TiO_2 powder with the dosage of 100 mg/L and KPS with different dosages (1~8 mM) were also added into the tube. For the kinetic analysis, the photodegradation of HBCD in the three systems of "UV/TiO_2 (TiO_2: 100 mg/L)", "UV/$K_2S_2O_8$ (KPS: 4 mM)", and "TiO_2 (TiO_2: 100 mg/L) + $K_2S_2O_8$ (KPS: 4 mM)" were performed, respectively. In all of the above experimental systems, after all the reagents were completely added, the mixed solution was placed in dark and stirred for 60 min to allow all the reagents to be uniformly mixed and to achieve adsorption equilibrium between TiO_2 particles (if any) and HBCD in the solution system. Then, turn on the cooling water and the 100 W mercury light source to start the photocatalytic reaction. Quickly take 2 mL of the sample at intervals of 30 min, place it in a tube containing 2 mL of methanol, mix well by shaking, and filter through a 0.22 μm filter. The filtrate was loaded into the sample vial for analysis in a liquid chromatograph. The average of 3 parallel determinations was taken as the concentration of each sample.

For the measurement of bromide ion concentration, a sample solution was quenched right after the sample was taken out by using a same volume of 0.2 M sodium nitrite solution. Then supernatant and the TiO_2 nanoparticles were separated in the same method. The supernatant was used to measure the concentration of bromide ion.

3.3. Analysis Method

Concentrations of HBCD were measured by a high-performance liquid chromatography (HPLC, LC-20AD, Shimadzu, Kyoto, Japan) instrument equipped with UV–vis detector set at 210 nm. The mobile phase was acetonitrile/water (85/15 (*v*/*v*)) and the flow rate was maintained at 1.0 mL/min. The HPLC chromatogram of HBCD was shown in Figure S2 (Supporting Information). According to the change of concentration of HBCD before and after degradation of the reaction system, the degradation rate of HBCD was calculated. The calculation was as follows:

$$\eta_{HBCD} = \frac{C_0 - C_t}{C_0} \times 100\% \tag{7}$$

where C_0 represents the initial concentration of HBCD in the reaction system and C_t represents the concentration of HBCD in the system at time t.

Concentration of bromide ion was measured by a Diane Ion chromatograph (ICS1100, Dionex, Sunnyvale, CA, USA) with an IonPac AS23 anion analytical column (250 mm × 4.0 mm × 5 μm, Dionex, Sunnyvale, CA, USA) and a Dionex IonPac AG22 anion protective column (50 mm × 4 mm, Dionex, Sunnyvale, CA, USA). The peak area-concentration standard curve of Br ion was plotted using potassium bromide powder as the bromine source. Leaching solution was 4.5 mM Na_2CO_3 and 1.4 mM $NaHCO_3$ with a flow rate of 1.2 mL/min.

The intermediates were qualitatively analyzed by a gas chromatography/mass spectrometry (GC/MS, Shimadzu QP2010 plus). The inlet temperature of GC is 200 degrees with the column type of DB-5MS capillary column (30 m × 0.25 mm × 0.25 μm, Agilent, Santa Clara, CA, USA). The injection volume is 1 μL, and the carrier gas is high purity nitrogen (99.999%). The ion source temperature, the electron bombardment energy, and the scanning mode of the mass spectrometer is 240 °C, 70 eV, and full scan mode (15~500 m/z), respectively. The sample solution was pretreated by extraction by dichloromethane and passed through anhydrous sodium sulfate, then it was concentrated by evaporation to about 1 mL under nitrogen, and passed through a 0.45 μm filter before the GC/MS analysis.

4. Conclusions

Degradation of HBCD is investigated in the UV/TiO_2, UV/KPS, and UV/TiO_2/KPS system by measurement of the concentrations of HBCD and bromide ion. HBCD can be almost completely degraded and 74.3% of the total bromine content is achieved in the UV/TiO_2/KPS homo/heterogeneous photocatalysis, much more than in the UV/KPS system and the UV/TiO_2

system. The $SO_4^{\bullet-}$ produced in persulphate and $OH^{\bullet}$ radicals produced in TiO_2 photocatalysis have synergistic effects in the degradation of HBCD in the UV/TiO_2/KPS homo/heterogeneous photocatalysis. The high yield of the concentration of bromide ions in the solutions indicates that fewer intermediates are formed in the UV/TiO_2/KPS homo/heterogeneous photocatalysis of HBCD. The efficient UV/TiO_2/KPS homo/heterogeneous system would provide great impetus to pollution control and environmental management.

Supplementary Materials: The following are available online at http://www.mdpi.com/2073-4344/9/2/189/s1, Figure S1: Photocatalysis for HBCD degradation in the UV/TiO_2/KPS system with three time cycling uses, Figure S2: The HPLC chromatogram of HBCD.

Author Contributions: Conceptualization, Q.L.; methodology, L.W.; formal analysis, L.Z.; investigation, X.F.; resources and data curation, J.L.; writing—original draft preparation, Q.L.; writing—review and editing, L.Z.; and H.X.

Funding: This research was funded by Natural Science Foundation of China (No. 21806101), Natural Science Foundation of Shanghai (Nos. 16ZR1412600, 15ZR1401200), Gaoyuan Discipline of Shanghai-Environmental Science and Engineering (Resource Recycling Science and Engineering), Innovation Research Grant (13YZ130) and Leading Academic Discipline Project (J51803) from the Shanghai Education Committee.

Conflicts of Interest: The authors declare no conflicts of interest.

References

1. Almughamsi, H.; Whalen, M.M. Hexabromocyclododecane and tetrabromobisphenol A alter secretion of interferon gamma (IFN-gamma) from human immune cells. *Arch. Toxicol.* **2016**, *90*, 1695–1707. [CrossRef] [PubMed]
2. Alaee, M.; Arias, P.; Sjodin, A.; Bergman, A. An overview of commercially used brominated flame retardants, their applications, their use patterns in different countries/regions and possible modes of release. *Environ. Int.* **2003**, *29*, 683–689. [CrossRef]
3. Jeannerat, D.; Pupier, M.; Schweizer, S.; Mitrev, Y.N.; Favreau, P.; Kohler, M. Discrimination of hexabromocyclododecane from new polymeric brominated flame retardant in polystyrene foam by nuclear magnetic resonance. *Chemosphere* **2016**, *144*, 1391–1397. [CrossRef] [PubMed]
4. Li, L.; Weber, R.; Liu, J.G.; Hu, J.X. Long-term emissions of hexabromocyclododecane as a chemical of concern in products in China. *Environ. Int.* **2016**, *91*, 291–300. [CrossRef]
5. Hunziker, R.W.; Gonsior, S.; Macgregor, J.A.; Desjardins, D. Fate and effect of hexabromocyclododecane in the environment. *Organohalogen Compd.* **2004**, *66*, 2300–2305.
6. Stiborova, H.; Vrkoslavova, J.; Pulkrabova, J.; Poustka, J.; Hajslova, J.; Demnerova, K. Dynamics of brominated flame retardants removal in contaminated wastewater sewage sludge under anaerobic conditions. *Sci. Total Environ.* **2015**, *533*, 439–445. [CrossRef] [PubMed]
7. Wagoner, E.R.; Baumberger, C.P.; Peverly, A.A.; Peters, D.G. Electrochemical reduction of 1, 2, 5, 6, 9, 10-hexabromocyclododecane at carbon and silver cathodes in dimethylformamide. *J. Electroanal. Chem.* **2014**, *713*, 136–142. [CrossRef]
8. Zhang, K.; Huang, J.; Wang, H.; Liu, K.; Yu, G.; Deng, S.B.; Wang, B. Mechanochemical degradation of hexabromocyclododecane and approaches for the remediation of its contaminated soil. *Chemosphere* **2014**, *116*, 40–45. [CrossRef] [PubMed]
9. Takigami, H.; Watanabe, M.; Kajiwara, N. Destruction behavior of hexabromocyclododecanes during incineration of solid waste containing expanded and extruded polystyrene insulation foams. *Chemosphere* **2014**, *116*, 24–33. [CrossRef] [PubMed]
10. Jondreville, C.; Cariou, R.; Meda, B.; Dominguez-Romero, E.; Omer, E.; Dervilly-Pinel, G.; Le Bizec, B.; Travel, A.; Baeza, E. Accumulation of a-hexabromocyclododecane (alpha-HBCDD) in tissues of fast- and slow-growing broilers (*Gallus domesticus*). *Chemosphere* **2017**, *178*, 424–431. [CrossRef]
11. Guo, Y.G.; Lou, X.Y.; Xiao, D.X.; Xu, L.; Wang, Z.H.; Liu, J.S. Sequential reduction-oxidation for photocatalytic degradation of tetrabromobisphenol A: Kinetics and intermediates. *J. Hazard. Mater.* **2014**, *241–242*, 301–306. [CrossRef] [PubMed]

12. Saien, J.; Ojaghloo, Z.; Soleymani, A.R.; Rasoulifard, M.H. Homogeneous and heterogeneous AOPs for rapid degradation of Triton X-100 in aqueous media via UV light, nano titania hydrogen peroxide and potassium persulfate. *Chem. Eng. J.* **2011**, *167*, 172–182. [CrossRef]
13. Salari, D.; Niaei, A.; Aber, S.; Rasoulifard, M.H. The photooxidative destruction of CI basic yellow 2 using UV/$S_2O_8{}^{2-}$ process in a rectangular continuous photoreactor. *J. Hazard. Mater.* **2009**, *166*, 61–66. [CrossRef] [PubMed]
14. Zhang, L.; Zhang, Q.H.; Xie, H.Y.; Guo, J.; Lyu, H.L.; Li, Y.G.; Sun, Z.G.; Wang, H.Z.; Guo, Z.H. Electrospun titania nanofibers segregated by graphene oxide for improved visible light photocatalysis. *Appl. Catal. B Environ.* **2017**, *201*, 470–478. [CrossRef]
15. Zhang, L.; Li, Y.G.; Xie, H.Y.; Wang, H.Z.; Zhang, Q.H. Efficient mineralization of toluene by W-doped TiO_2 nanofibers under visible light irradiation. *J. Nanosci. Nanotechnol.* **2015**, *15*, 2944–2951. [CrossRef]
16. Zhang, L.; Li, Y.G.; Zhang, Q.H.; Shi, G.Y.; Wang, H.Z. Fast synthesis of highly dispersed anatase TiO_2 nanocrystals in a microfluidic reactor. *Chem. Lett.* **2011**, *40*, 1371–1373. [CrossRef]
17. Aronne, A.; Fantauzzi, M.; Imparato, C.; Atzei, D.; De Stefano, L.; D′Errico, G.; Sannino, F.; Rea, I.; Pirozzi, D.; Elsener, B.; et al. Electronic properties of TiO_2-based materials characterized by high Ti^{3+} self-doping and low recombination rate of electron–hole pairs. *RSC Adv.* **2017**, *7*, 2373–2381. [CrossRef]
18. Sannino, F.; Pernice, P.; Imparato, C.; Aronne, A.; D′Errico, G.; Minieri, L.; Perfetti, M.; Pirozzi, D. Hybrid TiO_2–acetylacetonate amorphous gel-derived material with stably adsorbed superoxide radical active in oxidative degradation of organic pollutants. *RSC Adv.* **2015**, *5*, 93831–93839. [CrossRef]
19. Sannino, F.; Pernice, P.; Minieri, L.; Gamandona, G.A.; Aronne, A.; Pirozzi, D. Oxidative Degradation of Different Chlorinated Phenoxyalkanoic Acid Herbicides by a Hybrid ZrO_2 Gel-Derived Catalyst without Light Irradiation. *ACS Appl. Mater. Interfaces* **2015**, *7*, 256–263. [CrossRef]
20. Guo, Y.G.; Zhou, J.; Lou, X.Y.; Liu, R.L.; Xiao, D.X.; Fang, C.L.; Wang, Z.H.; Liu, J.S. Enhanced degradation of Tetrabromobisphenol A in water by a UV/base/persulfate system: Kinetics and intermediates. *Chem. Eng. J.* **2014**, *254*, 538–544. [CrossRef]
21. Neta, P.; Huie, R.E.; Ross, A.B. Rate constants of inorganic radicals in aqueous-solution. *J. Phys. Chem. Ref. Data* **1988**, *17*, 1027–1284. [CrossRef]
22. Xu, J.; Meng, W.; Zhang, Y.; Lei, L.; Guo, C.S. Photocatalytic degradation of tetrabromobisphenol A by mesoporous BiOBr: Efficacy, products and pathway. *Appl. Catal. B Environ.* **2011**, *107*, 355–362. [CrossRef]
23. Zhao, J.Y.; Zhang, Y.B.; Quan, X.; Chen, S. Enhanced oxidation of 4-chlorophenol using sulfate radicals generated from zero-valent iron and peroxydisulfate at ambient temperature. *Sep. Purif. Technol.* **2010**, *71*, 302–307. [CrossRef]
24. Li, Q.; Wang, L.F.; Zhang, L.; Xie, H.Y. Rapid degradation of tetrabromobisphenol A under the UV/TiO_2/KPS systems in alkaline aqueous solutions. *Res. Chem. Intermed.* **2018**. [CrossRef]
25. Ahmadi, M.; Ghanbari, F.; Moradi, M. Photocatalysis assisted by peroxymonosulfate and persulfate for benzotriazole degradation: Effect of pH on sulfate and hydroxyl radicals. *Water Sci. Technol.* **2015**, *72*, 2095–2102. [CrossRef] [PubMed]
26. Xie, H.Y.; Zhu, L.P.; Wang, L.L.; Chen, S.W.; Yang, D.D.; Yang, L.J.; Gao, G.L.; Yuan, H. Photodegradation of benzene by TiO_2 nanoparticles prepared by flame CVD process. *Particuology* **2011**, *9*, 75–79. [CrossRef]
27. Yang, H.; Zhou, S.L.; Yin, M.L.; Pi, L.L.; Zeng, J.; Yi, B. Parameters effect on photocatalytic kinetics of carbofuran in TiO_2 aqueous solution. *China Environ. Sci.* **2013**, *33*, 82–87.
28. Varanasi, L.; Coscarelli, E.; Khaksari, M.; Mazzoleni, L.R.; Minakata, D. Transformations of dissolved organic matter induced by UV photolysis, hydroxyl radicals, chlorine radicals, and sulfate radicals in aqueous-phase UV-Based advanced oxidation processes. *Water Res.* **2018**, *135*, 22–30. [CrossRef] [PubMed]
29. Li, W.; Jain, T.; Ishida, K.; Liu, H.Z. A mechanistic understanding of the degradation of trace organic contaminants by UV/hydrogen peroxide, UV/persulfate and UV/free chlorine for water reuse. *Environ. Sci. Water Res. Technol.* **2017**, *3*, 128–138. [CrossRef]
30. Elmolla, E.S.; Chaudhuri, M. Degradation of amoxicillin, ampicillin and cloxacillin antibiotics in aqueous solution by the UV/ZnO photocatalytic process. *J. Hazard. Mater.* **2010**, *173*, 445–449. [CrossRef] [PubMed]
31. Barontini, F.; Cozzani, V.; Cuzzola, A.; Petarca, L. Investigation of hexabromocyclododecane thermal degradation pathways by gas chromatography/mass spectrometry. *Rapid Commun. Mass Spectrom.* **2001**, *15*, 690–698. [CrossRef] [PubMed]

32. Zhou, D.N.; Chen, L.; Wu, F.; Wang, J.; Yang, F. Debromination of hexabromocyclododecane in aqueous solutions by UV-C irradiation. *Fresenius Environ. Bull.* **2012**, *21*, 107–111.
33. Yu, Y.; Zhou, D.; Wu, F. Mechanism and products of the photolysis of hexabromocyclododecane in acetonitrile–water solutions under a UV-C lamp. *Chem. Eng. J.* **2015**, *281*, 892–899. [CrossRef]
34. Zhao, Y.Y.; Zhang, X.H.; Sojinu, O.S. Thermodynamics and photochemical properties of alpha, beta, and gamma-hexabromocyclododecanes: A theoretical study. *Chemosphere* **2010**, *80*, 150–156.
35. Tso, C.P.; Shih, Y.H. The transformation of hexabromocyclododecane using zerovalent iron nanoparticle aggregates. *J. Hazard. Mater.* **2014**, *277*, 76–83. [CrossRef] [PubMed]